Self-extinguishing low-nitrogen nitrocellulose based on synergistic effect of dimethyl methylphosphonate and long-chain chlorinated paraffin

Xiaomei Yang[1)], Jingyu Wang[1)], Tianyou Song[1)], Zhipeng Li[1)], Jianwei Hao[1), *)]

DOI: dx.doi.org/10.14314/polimery.2018.6.3

Abstract: A series of flame retardant low-nitrogen nitrocelluloses (FR/NCs) containing different weight ratios of dimethyl methylphosphonate (DMMP) and long-chain chlorinated paraffin (CP) were directly prepared by blending method, and the burning behaviors, thermal and mechanical properties, pyrolysis process and char residues were investigated. The results showed that (DMMP/CP = 8/2)/NC at a total flame retardant loading of 17 wt % displayed the self-extinguishing behavior following a multi-flame retardancy mechanism with synergistic effect that includes gas-phase effects, endothermic effects and slightly condensed-phase effects of flame retardancy. In addition, the tensile properties of the (DMMP/CP = 8/2)/NC revealed a synergistic plasticization effect, which could enhance the flexibility of NC. This new system provided a reference for improving a safety storage and widely application of NC in the future.

Keywords: nitrocellulose, dimethyl methylphosphonate, chlorinated paraffin, multi-flame retardancy mechanism.

Samogasnąca nitroceluloza o małej zawartości azotu z dodatkiem synergicznie działających dimetylofosfonianu metylu i długołańcuchowej chlorowanej parafiny

Streszczenie: Metodą bezpośredniego mieszania składników otrzymano serię trudnopalnej nitrocelulozy o małym udziale azotu (NC) zawierającej dimetylofosfonian metylu (DMMP) zmieszany w różnych stosunkach masowych z długołańcuchową chlorowaną parafiną (CP). Oceniano właściwości palne, termiczne i mechaniczne wytworzonych mieszanin, badano również proces ich pirolizy, a także zwęgloną pozostałość po spaleniu. Stwierdzono, że mieszanina (DMMP/CP = 8/2)/NC z udziałem 17 % mas. uniepalniaczy charakteryzowała się zdolnością do samogaśnięcia w wyniku synergicznego wielofazowego mechanizmu uniepalniającego, obejmującego fazy gazową i częściowo skondensowaną, a także efekt endotermiczny. Dodatkowo właściwości wytrzymałościowe przy rozciąganiu wspomnianej mieszaniny wskazywały na synergiczne działanie plastyfikujące zastosowanych związków uniepalniających. Opracowana mieszanina pozwala na zwiększenie bezpieczeństwa przechowywania i użytkowania nitrocelulozy.

Słowa kluczowe: nitroceluloza, dimetylofosfonian metylu, chlorowana parafina, wielofazowy mechanizm uniepalniania.

Nitrocellulose (NC) is one of the most promising green polymers, which has a wide range of applications such as propellants [1], passivation layer [2], coatings [3], printing inks [4] and sensor [5]. Typically, NC with low nitrogen contents is extensively used as nitro lacquer due to its high transparency and fast drying [6]. However, the application of NC is restricted in many chemical industry because of its high sensitivity for flammability [7], especially for the spontaneous self-combustion in bulk storage [8]. One typical disastrous accident involving NC occurred in Tianjin Port in China on 12 August 2015, in which two severe explosions were triggered, causing 165 deaths, 798 injuries, and 8 missing [9]. In addition, the poor mechanical properties of NC (because NC possesses semi-rigid structure) also restrict its widespread use [10]. Due to these disadvantages, it is necessary to introduce some compounds, including highly effective flame retardants and plasticizers in order to protect the safety storage and to broaden the applications of NC.

[1)] Beijing Institute of Technology, School of Materials Science and Engineering, National Engineering Technology Research Center of Flame Retardant Materials, Beijing 100081, PR China.

[*)] Authors for correspondence; e-mail: hjw@bit.edu.cn

Recently, our group has made some contribution to the improvement of thermal stability of NC [11, 12], however, no relevant literature on enhancing the flame retardancy of NC for satisfying its further safe needs was found.

Among the commercially available flame retardants, the phosphorus-containing compounds are often used as additives for polymer to modify its flammability and participate in the gas-phase effect and/or condensed-phase [13, 14]. The liquid flame retardant dimethyl methylphosphonate (DMMP) with an advantage of high phosphate content (> 25 %) and low decomposition temperature (180 °C) may be a suitable choice for NC. It can generate PO_2 and PO free radicals to scavenge H and OH free radicals released by polymer, which presents gas-phase mechanism during combustion [15, 16], and it also can form several phosphorus-containing acids to accelerate the formation of protective layer [17]. Furthermore, the toughness of NC may be improved because DMMP can be used as a plasticizer [18].

Chlorinated paraffin (CP) is another kind of flame retardant and plasticizer additive. The short-chain CP has been highly regarded as a candidate compound for persistent organic pollutants (POPs) in the Stockholm Convention due to bioaccumulation and toxicity. While, the long-chain (≥ C18) CP, for example CP-70, has not been limited by international regulations [19]. Furthermore, CP with high contents of C-H, may have the ability to provide a carbon source as a carbonaceous agent for NC. In recent years, more and more researches are focused on the low cost and high efficiency flame retardants with the synergistic effect. Since DMMP and CP play the flame retardant roles by different mechanisms, it is expected that DMMP with phosphorus and CP with chlorine simultaneously added into NC may produce the synergistic effect of flame retardancy. According to this assumption, we will introduce low cost flame retardant DMMP, CP and their mixture into NC, and then in detail explore their thermal behaviors, and the probable flame retardancy mechanism as well as the mechanical properties.

EXPERIMENTAL PART

Materials

NC (nitrogen content ~ 11.91 wt %) was kindly provided by Baoding BaoFeng Nitrocellulose Co., Ltd., Hebei, China. DMMP was supplied by Plastic Chemical Technology Co., Ltd., Guangdong, China. CP (CP-70, content of Cl ≥ 70 %) was purchased from Jinan Taixing Fine Chemical Co., Ltd., Shandong, China. *n*-Butyl acetate (BAC, AR) was purchased from Tianjin Guangfu Technology Development Co., Ltd, China. NC was pre-treated in a freeze dryer at -80 °C for 48 h to remove residual water and then stored in desiccators before use.

Preparation of samples

NC was dissolved in BAC totally by agitation, and transferred into ultrasonic treatment to remove the air bubbles. Finally, the NC solution was poured into polytetrafluoroethylene mold [100 × 100 × 5 (mm^3)], dried at ambient temperature for 24 h. Then the residual solvents were removed in oven for 48 h at 60 °C to obtain a homogeneous membrane of NC. Flame retardant low-nitrogen nitrocelluloses (FR/NCs) were prepared with the same method. The only difference was that the DMMP and CP were dissolved into BAC by ultrasonic dispersion in advance, and then incorporated into NC solution with the different weight ratios as shown in Table 1.

Methods of testing

– Limiting oxygen index (*LOI*) was measured by a FTA-II instrument (Rheometric Scientific Ltd.) with specimen dimensions of 90 × 10 × 0.5 (mm^3). *LOI* values were judged just by ensuring the samples burn to ~ 60 mm after igniting.

– Horizontal burning test (HB) was carried out using a CZF-3 instrument (Jiangning Analysis Instrument Factory) with specimen dimensions of 90 × 10 × 1 (mm^3), and

T a b l e 1. Limiting oxygen index (*LOI*) and horizontal burning test (HB) of NC and FR/NCs containing 17 wt % of FR

No.	Formulation					Flame retardancy		
	Sample	NC wt %	DMMP wt %	CP wt %	DMMP/CP	*LOI* %	Burning rate mm/min	Rating
1	NC	100	–	–	–	17.6	900	No
2	CP/NC	83	–	17.0	–	21.6	600	No
3	DMMP/CP/NC	83	3.4	13.6	2/8	20.3	600	No
4	DMMP/CP/NC	83	5.1	11.9	3/7	20.4	600	No
5	DMMP/CP/NC	83	8.5	8.5	5/5	22.0	510	No
6	DMMP/CP/NC	83	11.9	5.1	7/3	24.7	42	HB [20]
7	DMMP/CP/NC	83	13.6	3.4	8/2	28.4	0	HB [20]
8	DMMP/NC	83	17.0	–	–	21.7	516	No

the results were calculated and presented according to the burning rate and the rating. A material classed HB shall not have a burning rate exceeding 75 mm/min over a 75 mm span for specimens having a thickness less than 3.0 mm [20].

– Cone calorimeter (CONE) measurements were performed with a fire testing technology apparatus under 15 kW/m^2 external radiant heat flux conforming to ISO 5660 protocol. The specimen dimensions were 100 × 100 × 1 (mm^3) for each sample. The main parameters were obtained: time to ignition (*TTI*), peak of heat release rate (*PHRR*), total heat release (*THR*), index of fire performance (*FPI*) and average effective heat of combustion (Av-*EHC*).

– Thermogravimetric analysis-differential scanning calorimeter (TGA-DSC) was performed on a thermal analyzer (Mettler-Toledo) with a continuous flow of nitrogen atmosphere at a heating rate of 10 °C/min from 50 to 300 °C. The following parameters were determined: initial decomposition temperature based on 5 % weight loss ($T_{5\,\%}$) and char residues at 300 °C ($CR_{300\,°C}$). The theoretical char residues values of (DMMP/CP = 8/2)/NC and DMMP/CP = 8/2 were calculated according to following equation:

$$W_{cal}(T) = \sum_{i=1}^{n} X_i W_i(T) \quad (1)$$

where: X_i – the corresponding weight contents, W_i – the corresponding experimental char residues.

– Thermogravimetric analysis-Fourier transform infrared spectrometry (TGA-FTIR) (Nicolet 6700) was used to detect pyrolysis gas products, and the measurement was carried out under nitrogen atmosphere at a heating rate of 20 °C/min from 40 °C to 400 °C. The sample weight was ~ 10 mg for each measurement.

– The morphology of the surface char residues after horizontal burning test was determined by scanning electron microscopy (SEM) (TM3000 and Hitachi S-4700). In addition, the membranes were quenched and fractured in liquid nitrogen to prepare the samples for the examination of fracture surface morphology by SEM.

– Elemental compositions and contents of char residues after horizontal burning test were determined from X-ray photoelectron spectroscopy (XPS) (PHI Quantera II SXM) under a vacuum of 2.6 · 10^{-7} Pa with AlKα X-ray source at 25 W. The spectrometer was calibrated using the binding energy of adventitious carbon as 284.6 eV.

– Graphitization degree of char residues after horizontal burning test was measured by Laser Raman spectroscopy analysis (Renishaw inVia^{TM}). The resolution of the Raman instrument was approximately 4 cm^{-1}. The excitation source is a 514 nm argon ion gas laser and the output power is 20 mW.

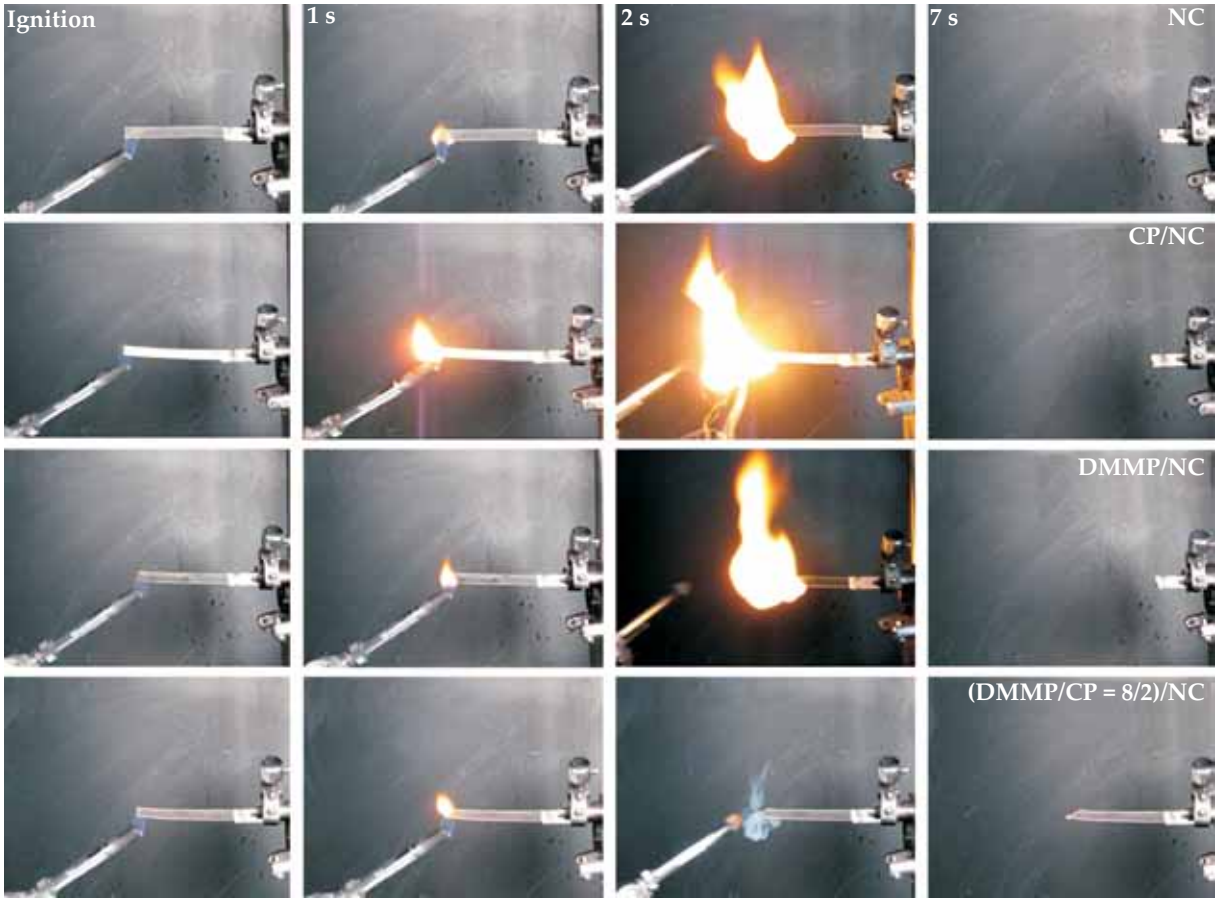

Fig. 1. Horizontal burning processes of NC and FR/NCs containing 17 wt % of FR at different time

– Dynamic mechanical analysis (DMA) was carried out using a dynamic mechanical analyzer (Rheometric Scientific DMTA V). The dimensions of the specimens were 6 × 5 × 1 (mm^3). The measuring frequency was 1 Hz. The temperature was varied in the range 20–180 °C with a heating rate of 3 °C/min.

– Rectangular tensile bars measuring 50 × 10 × 0.1 (mm^3) were obtained using a fresh razor blade. Uniaxial tensile tests (INSTRON 1185) were carried out at 25 °C with a crosshead speed of 5 mm/min. The moduli were determined by linearly fitting the elastic portion of the stress-strain curves, and the results were the averages of 5 measurements.

RESULTS AND DISCUSSION

Burning behaviors

The burning behaviors of NC and FR/NCs with different weight ratios of DMMP and CP were evaluated in terms of *LOI* and HB test. The results are summarized in Table 1 and the horizontal burning processes are recorded in Fig. 1.

Generally speaking, materials exhibiting *LOI* value above 26 % will show self-extinguishing behavior in air and are considered to possess high flame retardancy [21]. Pure NC (Sample 1, burning rate of 900 mm/min, see Table 1) shows high combustion, and its *LOI* value is only 17.6 %. CP or DMMP alone can slightly increase the *LOI* value of NC system, but CP/NC (Sample 2, burning rate of 600 mm/min, see Table 1) or DMMP/NC (Sample 8, burning rate of 516 mm/min, see Table 1) cannot pass the HB test (can't reach HB rating), which demonstrates that neither CP nor DMMP exerts an obvious influence on the flame retardancy of NC. However, with the increasing content of DMMP and the decreasing content of CP in FR at a constant FR loading of 17 wt % in NC, the *LOI* value of (DMMP/CP = 8/2)/NC presents a maximum value of 28.4 %, and the sample reaches HB rating (Sample 7, burning rate of 0 mm/min, see Table 1). Notably, there is a phosphorus-chlorine synergistic effect of flame retardancy between DMMP and CP with the weight ratio of 8/2.

In order to simplify the analytical process, we just took NC, CP/NC, DMMP/NC and (DMMP/CP = 8/2)/NC to examine the synergistic effect of flame retardancy and its mechanism, and do not mention the other samples any longer.

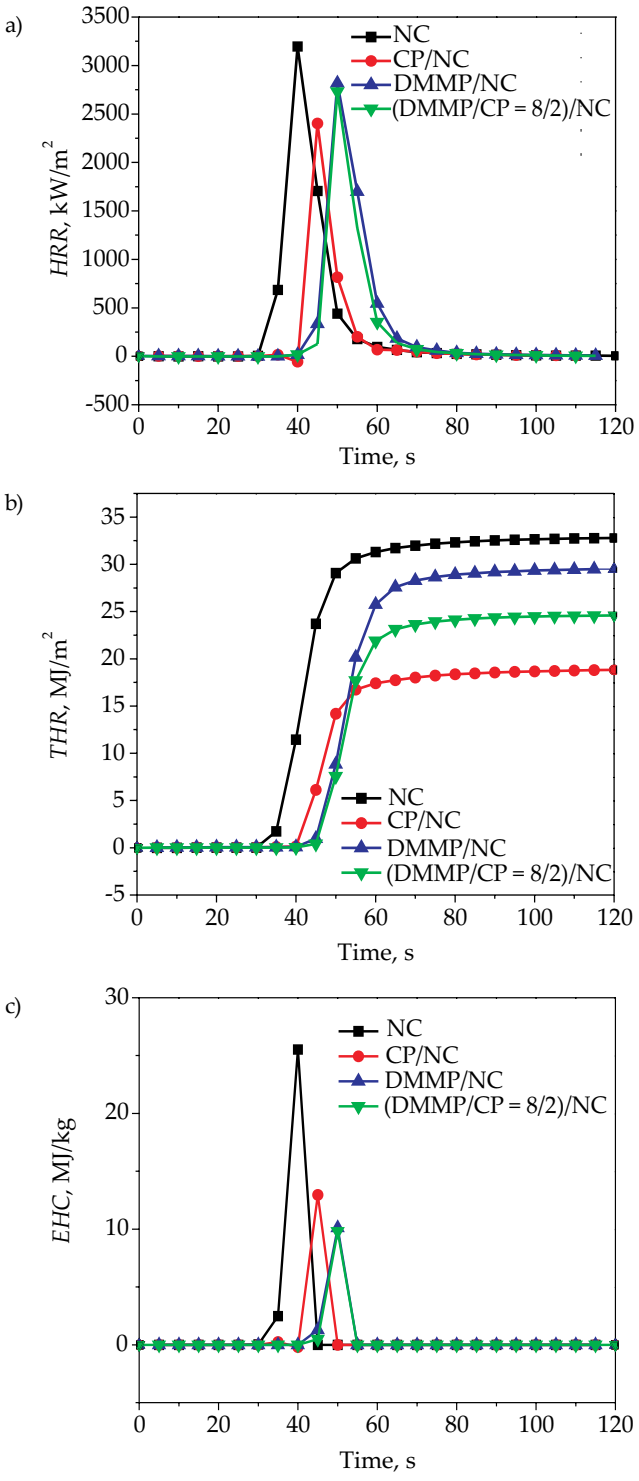

Fig. 2. a) *HRR*, b) *THR*, c) *EHC* curves of NC and FR/NCs containing 17 wt % of FR

T a b l e 2. Cone calorimetry data of NC and FR/NCs containing 17 wt % of FR

Sample	*PHRR* kW/m²	*TTI* s	*THR* MJ/m²	*FPI* m²s/kW	Av-*EHC* MJ/kg
NC	3197	27	32.7	0.008	5.6
CP/NC	2403	34	18.8	0.014	2.6
DMMP/NC	2818	40	29.5	0.014	2.3
(DMMP/CP = 8/2)/NC	2732	40	24.5	0.015	2.0

T a b l e 3. TGA and DSC data of NC, (DMMP/CP = 8/2)/NC, DMMP/CP = 8/2, DMMP and CP

Sample	TGA				DSC	
	$T_{5\,\%}$ °C	Char residues %	$R_{DMMP/CP/NC}$ %	$R_{DMMP/CP}$ %	T_d °C	Exothermic energy, J/g
NC	176.4	1.2	—	—	184.6	248.14
(DMMP/CP = 8/2)/NC	172.1	1.6	4.2	—	179.9	163.96
DMMP/CP = 8/2	68.7*	18.9	—	18.8	139.8	-98.66
DMMP	60.2*	0.1	—	—	135.7	-102.38
CP	297.0	94.3	—	—	—	—

R – theoretical values of char residue,
* 5 wt % volatilization temperatures.

CONE is used to evaluate realistically burning behavior of polymer and to study the flammability properties of materials. Some of the important parameters derived from CONE are shown in Table 2, and the *HRR*, *THR* and *EHC* curves are shown in Fig. 2.

NC has the high *PHRR* value (3197 kW/m^2), which is far higher than that of polypropylene PP (1192 kW/m^2) [22], polycarbonate PC (528 kW/m^2) [23], high impact polystyrene HIPS (738 kW/m^2) [24], medium density polyethylene MDPE (1090 kW/m^2) [25] and high density polyethylene HDPE (1146 kW/m^2) [26], indicating the NC is a kind of extremely flammable material. In addition, the *TTI*, *THR*, and Av-*EHC* of NC are 27 s, 32.7 MJ/m^2 and 5.6 MJ/kg, respectively. After introducing FR, the *TTI* is delayed, the *PHRR*, *THR* and Av-*EHC* values of FR/NCs are decreased. Those results suggest that the FR could reduce the surface heat and the amount of volatile combustibles, and decrease the risk connected with NC accordingly. *FPI* is defined as the proportion of the *TTI* to the *PHRR* [27]. As reported, the higher the *FPI*, the lower the fire danger (*i.e.*, the time to flash burning is longer) [28]. As shown in Table 2, the *FPI* values of FR/NCs are all increased by one order of magnitude compared with that of NC (0.008 m^{2}s/kW). Typically, the (DMMP/CP = 8/2)/NC possesses the highest value of *FPI* (0.015 m^{2}s/kW), indicating the best flame retardancy with the phosphorus-chlorine synergistic effect. Av-*EHC* is often used to assess the amount of the effective burning component of materials in the gas-phase [29], and a higher Av-*EHC* value means a more completely combustion of volatiles [30]. As shown in Fig. 2c and Table 2, the Av-*EHC* values of FR/NCs are all reduced obviously to that of NC (5.6 MJ/kg), and the most obvious reduction of Av-*EHC* for (DMMP/CP = 8/2)/NC (2.0 MJ/kg) can illustrate the gas-phase synergistic effect of flame retardancy. These results are consistent with the results of *LOI* and HB.

Thermal behaviors and pyrolysis process

Thermal behaviors of NC, (DMMP/CP = 8/2)/NC, DMMP/CP = 8/2, DMMP and CP under nitrogen atmosphere are recorded by TGA (Fig. 3a) and DSC (Fig. 3b). All the corresponding data are presented in Table 3.

From the Fig. 3a and Table 3, temperatures for 5 wt % weight loss ($T_{5\,\%}$) of CP is 297.0 °C; 5 wt % volatilization temperatures of DMMP/CP = 8/2 and DMMP are 68.7 °C and 60.2 °C, respectively. This indicates that DMMP will enter gas-phase at a low temperature. Both the $T_{5\,\%}$ (172.1 °C, obtained from TGA) and the exothermic peak temperature (T_d) (179.9 °C, obtained from DSC) of (DMMP/CP = 8/2)/NC are lower than the $T_{5\,\%}$ (176.4 °C) and the T_d (184.6 °C) of NC, respectively. This is because the (DMMP/CP = 8/2)/NC sample contains unsta-

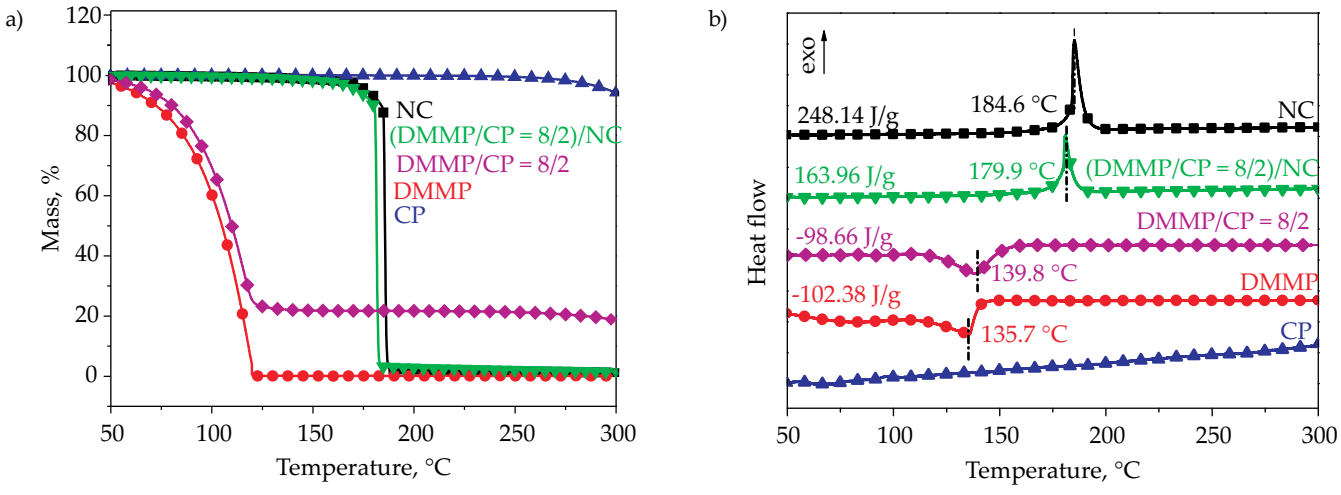

Fig. 3. a) TGA, b) DSC curves of NC, (DMMP/CP = 8/2)/NC, DMMP/CP = 8/2, DMMP and CP

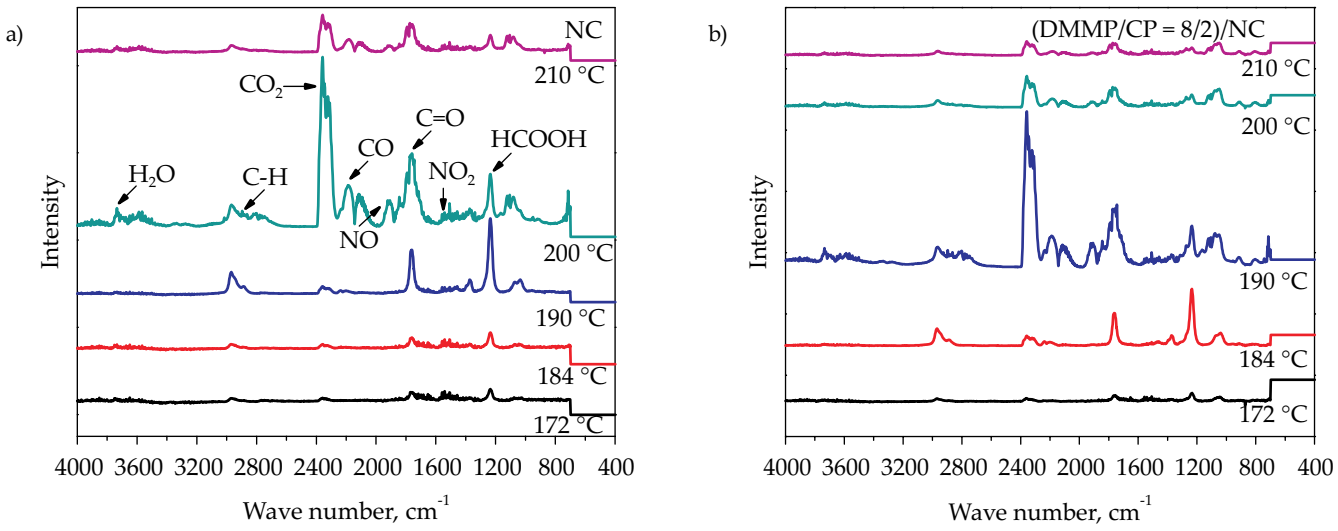

Fig. 4. TGA-FTIR spectra of pyrolysis products of: a) NC, b) (DMMP/CP = 8/2)/NC containing 17 wt % of DMMP/CP during the thermal degradation at different temperature

ble P-O-C bond, leading to the thermal decomposition of flame retardant in advance [31], and plays the role in gas-phase effect of flame retardancy. In addition, the experimental char residue value of (DMMP/CP = 8/2)/NC at 300 °C is 1.6 %, which is slightly higher than that of NC (1.2 %), while far lower than that of its theoretical char residues value (4.2 %), further indicating the gas-phase effect of flame retardancy. What is more, there is almost no obviously condensed-phase effect of flame retardancy according to the result that the theoretical char residues value of DMMP/CP = 8/2 (18.8 %) is close to that of experimental char residues value (18.9 %). As shown in Fig. 3b and Table 3, the exothermic energy of (DMMP/CP = 8/2)/NC is decreased by 33.9 % from 248.14 J/g of NC because of the endothermic energy of DMMP/CP = 8/2 (98.66 J/g), that mainly is derived from endothermic energy of DMMP (102.38 J/g). These results indicate that the DMMP/CP = 8/2 can absorb part of instantaneous exothermic energy of NC, inhibit the heat release and reduces the susceptibility of NC to thermal decomposition. Thus, the flame retardancy mechanism of (DMMP/CP = 8/2)/NC might mainly belong to gas-phase and endothermic effects of flame retardancy.

In order to explore the gas-phase mechanism and obtain the information about the pyrolysis gas products, the TGA-FTIR spectra of NC and (DMMP/CP = 8/2)/NC during the thermal degradation at different temperature are shown in Fig. 4a and Fig. 4b, respectively.

It can be seen that the major pyrolysis gases resulting from the decomposition process are H_2O (3584–3740 cm^{-1}), CO_2 (2360 cm^{-1}), CO (2111, 2184 cm^{-1}), hydrocarbons (2814 cm^{-1}), NO (1910 cm^{-1}), NO_2 (1567 cm^{-1}), C=O (1767 cm^{-1}) and HCOOH (1237 cm^{-1}), which correspond well with the decomposition gas products of NC reported in the literature [32, 33]. Clearly, the pyrolysis products of (DMMP/CP = 8/2)/NC are released earlier than that of NC, which can be attributed to the loss of DMMP at low temperature. Figure 5 shows the FT-IR spectra of pyrolysis products of NC and (DMMP/CP = 8/2)/NC at the maximum decomposition temperature. The latter sample shows several new small peaks near 806 cm^{-1}, 918 cm^{-1}, 1060 cm^{-1} and 1161 cm^{-1}, 1284 cm^{-1} and 1321 cm^{-1}, which correspond with the P-O [34], P-O-C [35], PO_2 [34], P=O [36, 37] and CH_3-P [37, 38], respectively, from the decomposition of DMMP. Furthermore, the peak near 2885 cm^{-1} contains absorption band of HCl, that is released by CP, which may overlap with C-H bands of NC and CP. Figure 6 shows the absorbance of pyrolysis products of NC and (DMMP/CP = 8/2)/NC calculated per milligram of sample during the thermal degradation process. The characteristic peaks of H_2O, alkanes and carbonyl compounds of (DMMP/CP = 8/2)/NC appear earlier than that of NC, further confirming the earlier decomposition of (DMMP/CP = 8/2)/NC, as showed in Fig. 4. This phenomenon suggests that the

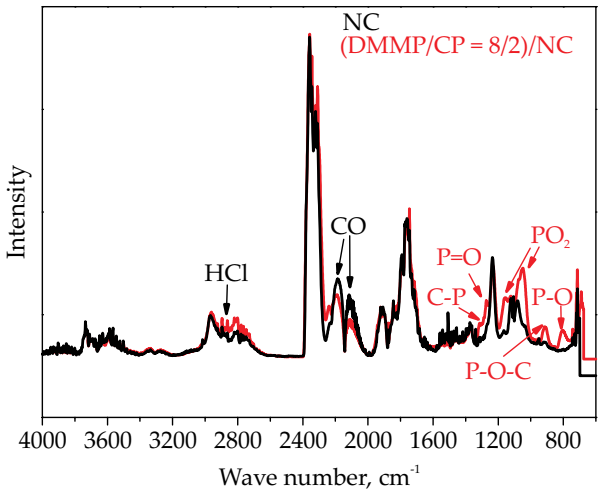

Fig. 5. FT-IR spectra of pyrolysis products of NC and (DMMP/CP = 8/2)/NC containing 17 wt % of DMMP/CP at the maximum decomposition temperature

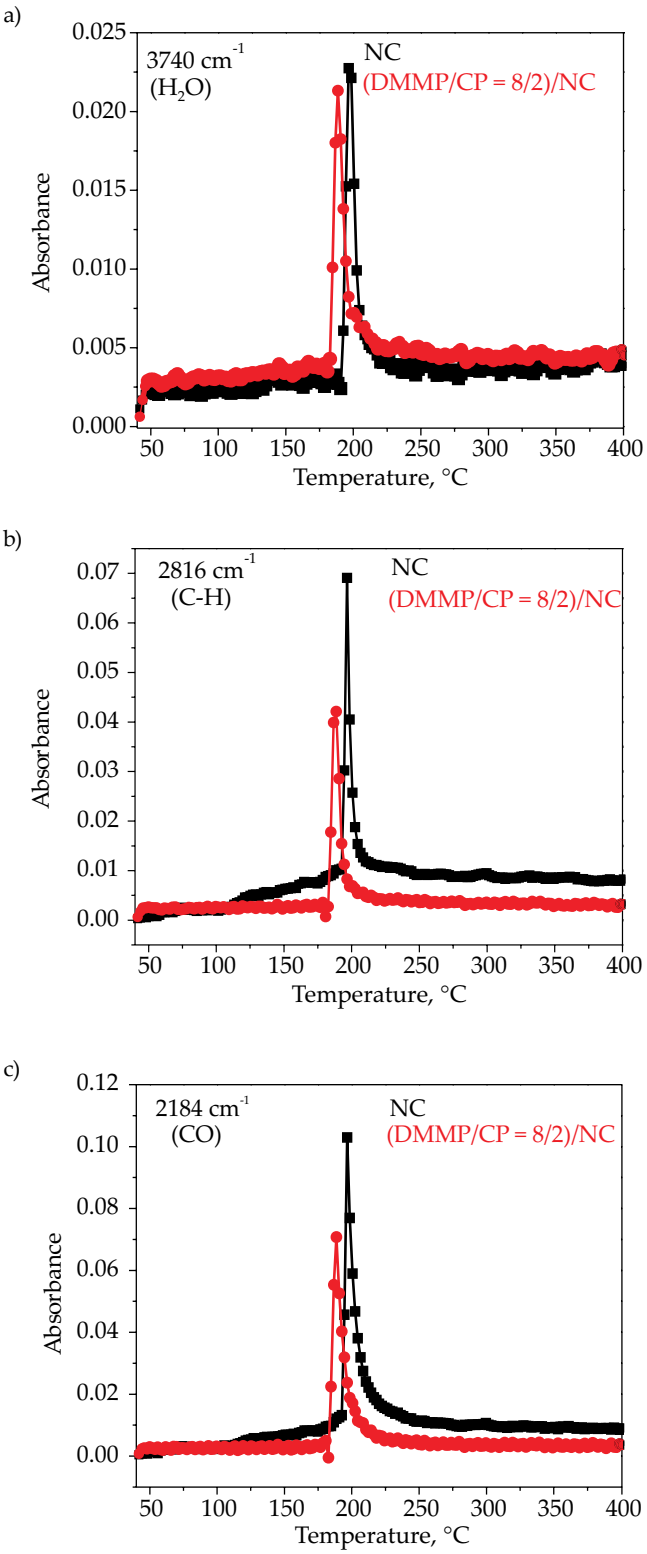

Fig. 6. Absorbance of pyrolysis products for NC and (DMMP/CP = 8/2)/NC containing 17 wt % of DMMP/CP: a) H_2O, b) C-H, c) CO

(DMMP/CP = 8/2)/NC decomposes at lower temperature and accelerates the dehydration action, thus protecting the NC from being attacked by flames [39]. In addition, the lower release of combustion gases (Fig. 6) indicates the lower heat release rate for NC, which proves the improvement of the flame retardancy of NC. Based on the above facts, it can be concluded that the PO_2 and PO free radicals produced by DMMP and HCl released by CP, quench the active free radicals from the NC matrix; furthermore, the HCl can inhibit the burning process and dilute the O_2 resulting in the improvement of the flame retardancy of NC. Therefore, combining with the results of *LOI*, HB, CONE and TGA-DSC, we conclude that both of DMMP and CP play the roles in the gas-phase effect of flame retardancy, and when the weight ratio of DMMP/CP is 8/2, its effect of flame retardancy will be maximized.

Char residues

It is well-known that the char structure is one of the most important factors to determine the flame retardancy. Figure 7 illustrates the digital photograph and the SEM images of char residues of NC and (DMMP/CP = 8/2)/NC after the horizontal burning test. It can be seen that only loose char residues (Fig. 7a, Fig. 7c) are remained for NC where the heat and flammable volatiles can penetrate easily during combustion. The morphology of char residues for (DMMP/CP = 8/2)/NC, however, is very different from the NC, and a lot of hard, brittle charred solid (Fig. 7b) and the compact layer structures (Fig. 7d) are observed. These results may be attributed to the formation of solid char layer of both CP that plays its role in condensed-phase [40, 41] and phosphoric acid/poly(metaphosphoric acid) analogues derived from the decomposition of DMMP [18]. The solid char layer covers onto the NC matrix to protect the NC from burning further. Therefore, it can be predicted that DMMP combined with CP in NC matrix will also have a slightly condensed-phase effect of flame retardancy, which will play a positive role in self-extinguishing behavior to some extent.

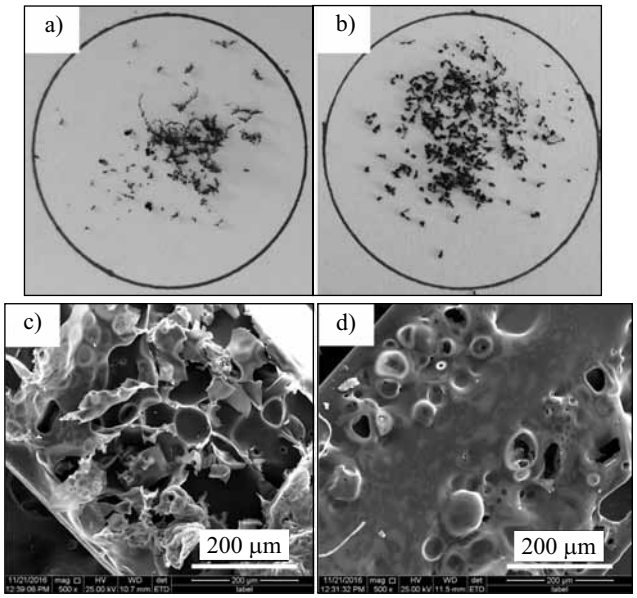

Fig. 7. Digital photograph of char residues of: a) NC, b) (DMMP/CP = 8/2)/NC; surface SEM images of char residues of: c) NC, d) (DMMP/CP = 8/2)/NC

XPS curves obtained for char residues of the above two samples are shown in Fig. 8a. The spectrum of (DMMP/CP = 8/2)/NC char residue shows additional signals of chlorine (201.2 eV, Cl 2p, 1.08 %) and phosphorus (134.5 eV, P 2p, 1.41 %), respectively, indicating that the CP and DMMP are retained in the char residue and participate in the condensed-phase effect of flame retardancy. Raman spectra (Figs. 8b and 8c) were used to investigate the graphitic char structure for the above two samples. The spectra are fitted to D band (around 1384 cm^{-1}) that corresponds to unorganized carbon structure and G band (around 1571 cm^{-1}) that associates with hexagonal graphitic structure [42]. The intensity ratio of D and G bands (A_D/A_G) is indicative of graphitization degree of the char [43]. Generally, the lower A_D/A_G corresponds to the formation of higher graphitization degree carbonaceous materials [44]. The A_D/A_G value of (DMMP/CP = 8/2)/NC (5.94) is lower than that of NC (6.65). It illustrates that more thermally stable graphitic char is formed for (DMMP/CP = 8/2)/NC sample due to the dehydrochlorination of CP, which enhances the graphitic barrier function and results in more marked flame retardancy of NC accordingly.

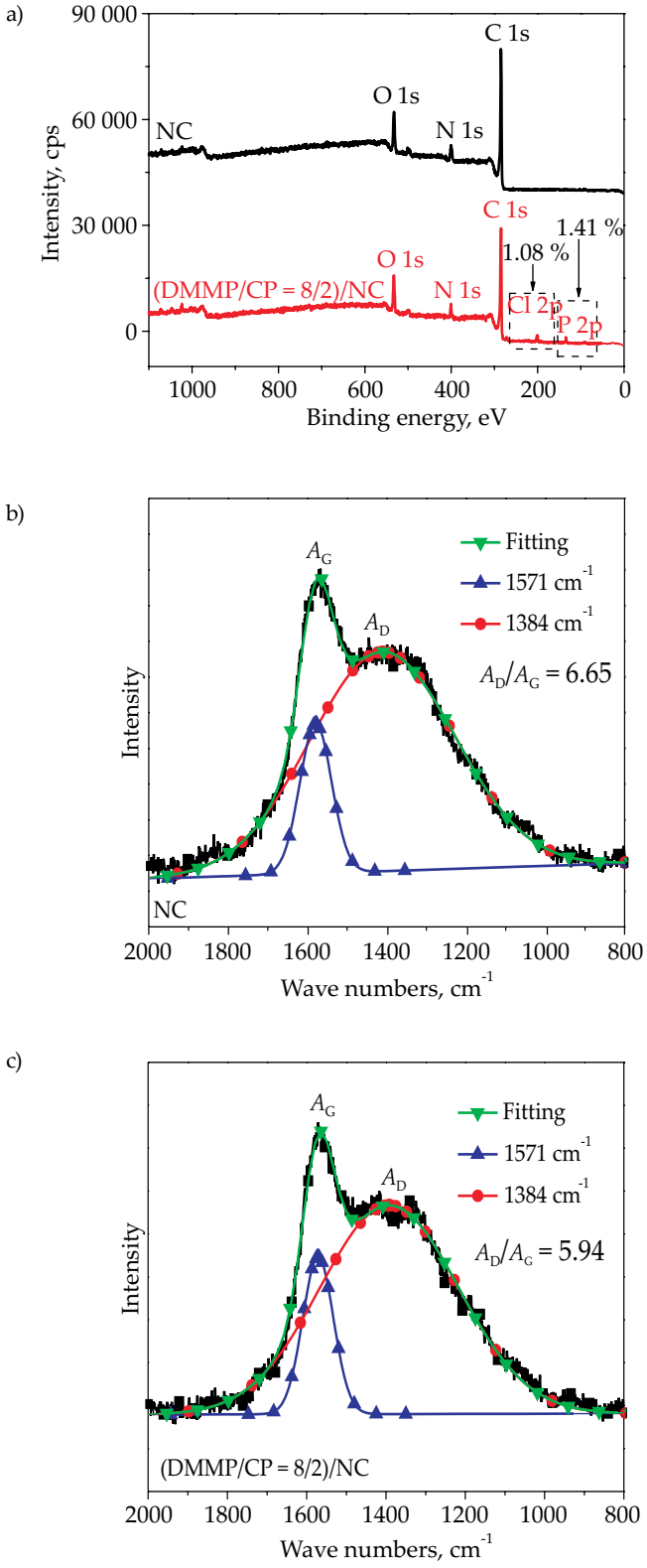

Fig. 8. a) XPS spectra of NC and (DMMP/CP = 8/2)/NC char residues, b) Raman spectra of NC char residues, c) Raman spectra of (DMMP/CP = 8/2)/NC char residues

Multi-flame retardancy mechanism

From the above results, the phosphorus-chlorine synergistic effect promotes the flame retardancy of (DMMP/CP = 8/2)/NC significantly, which is reflected by the increase of *LOI* value, reaching the HB rating, the increase of *FPI* value and the decrease of Av-*EHC* value. Thereafter, the flame retardancy mechanism is proposed and illustrated in Fig. 9. As mentioned above, NC combusts drastically after ignition; while, the self-extinguishing phenomenon is observed for (DMMP/CP = 8/2)/NC after removing the igniter. There are some complex reasons. Firstly, DMMP is considered to act mainly in gas-phase. The PO and PO_2 free radicals that are released from DMMP can capture the ignitable HO, O and H free radicals from NC matrix [45, 46]. HCl gases that are released by CP can also capture the ignitable HO, O and H free radicals, and then dilute some combustion energy and O_2. Furthermore, the emission of gaseous products through vaporization of DMMP can absorb part of exothermic energy of instantaneous combustion of NC. Secondly, the DMMP perhaps produces some phosphoric acid/poly(metaphosphoric acid) analogues that cover onto NC matrix by acting as a barrier to restrain heat exchange and further burning. Accordingly, the heated CP begins to form hard and discontinuous char residues to eliminate the thermal energy and insulate the heat transmission from fire and heat conduction, further keeping the NC matrix from heat and degradation. The (DMMP/CP = 8/2)/NC system not only captures the ignitable alkyl free radicals, decreases the exothermic energy, dilutes some combustion energy and O_2, but also inhibits the thermal feedback of the NC matrix. All the effects of flame retardancy are combined together to produce better flame retardancy behavior. Therefore, we confirmed that the flame retardancy of (DMMP/CP = 8/2)/NC is not due to any single mechanism but rather a multi-flame retardancy mechanism

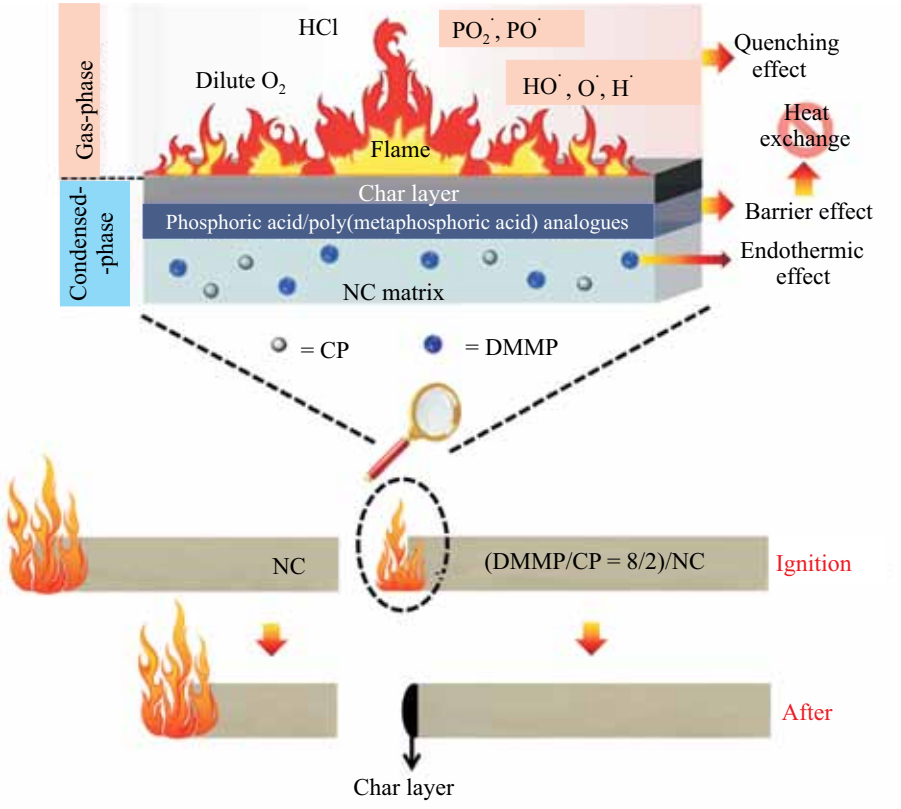

Fig. 9. The probable phosphorus-chlorine synergistic multi-flame retardancy mechanism

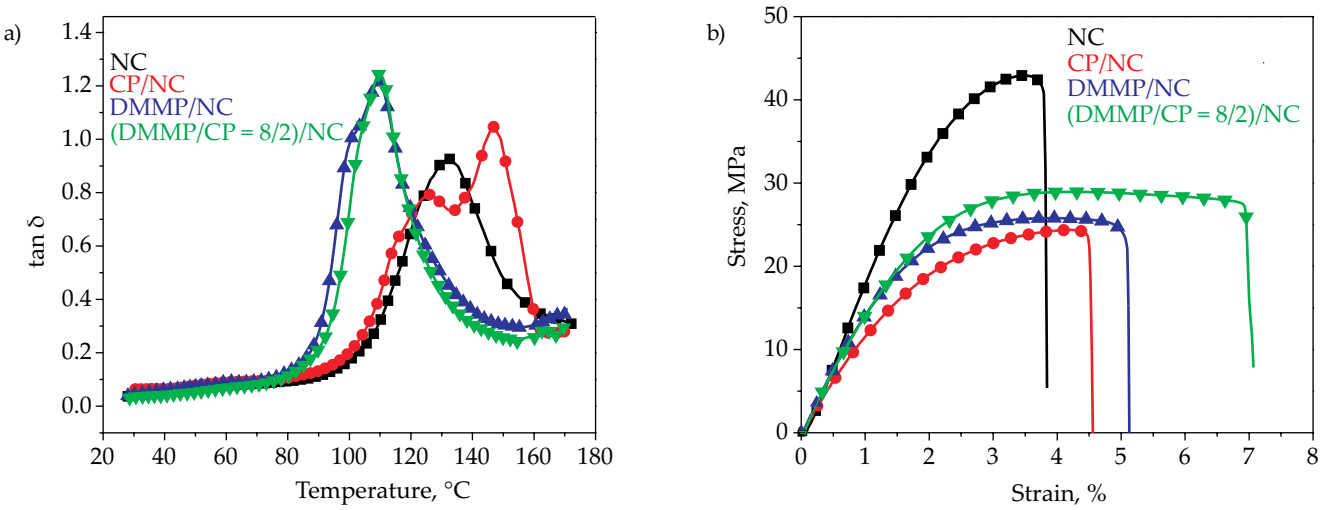

Fig. 10. a) tan δ curves, b) stress-strain curves of NC and FR/NCs containing 17 wt % of FR

T a b l e 4. Mechanical properties of NC and FR/NCs containing 17 wt % of FR

Sample	Tensile modulus MPa	Tensile strength MPa	Elongation at break %
NC	1953 ± 102	42.9 ± 1.2	3.84 ± 0.32
CP/NC	1373 ± 147	24.4 ± 1.9	4.56 ± 0.78
DMMP/NC	1544 ± 125	25.8 ± 3.2	5.13 ± 0.81
(DMMP/CP = 8/2)/NC	1664 ± 113	28.9 ± 2.6	7.07 ± 0.56

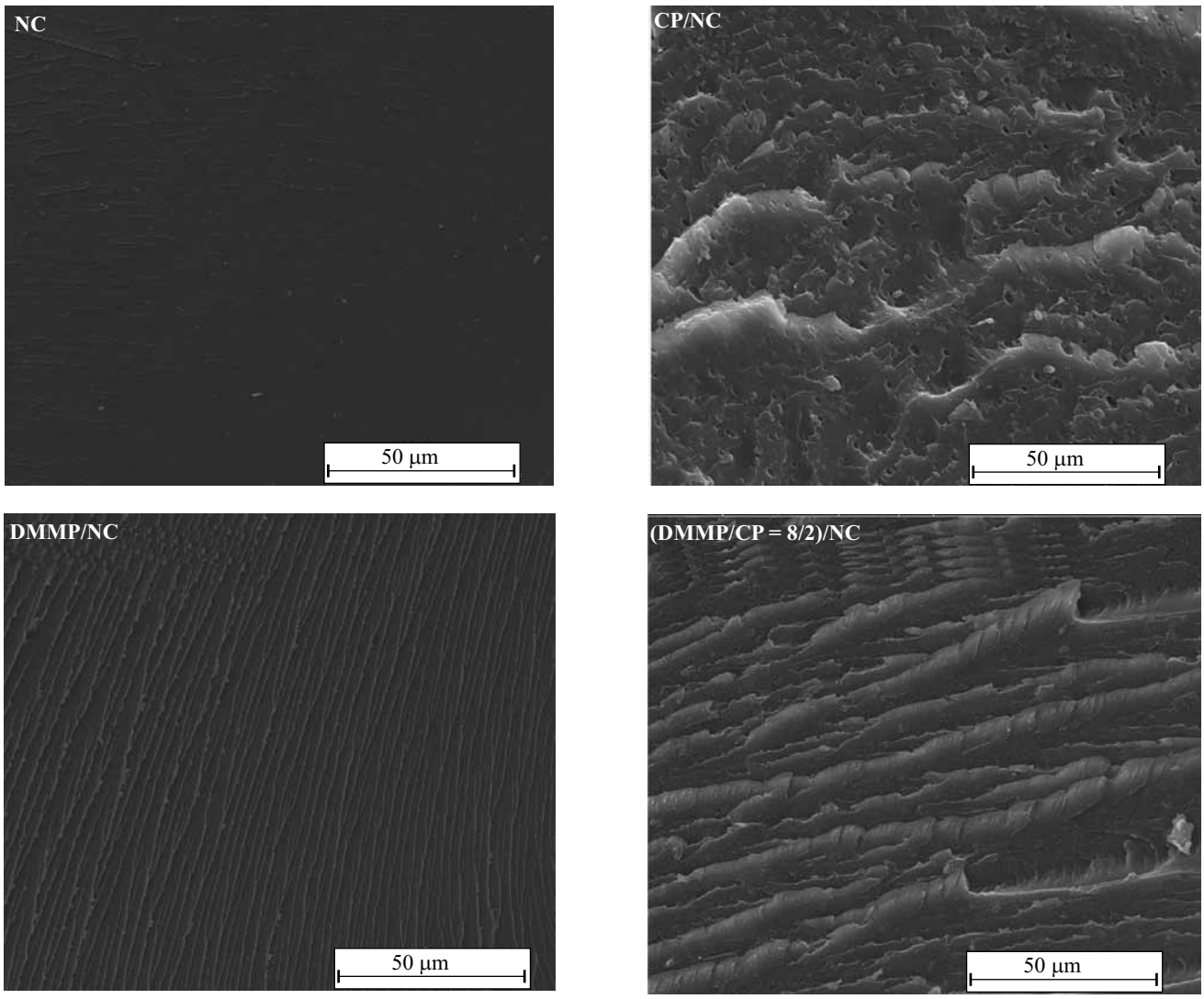

Fig. 11. SEM images of fracture surface for NC and FR/NCs containing 17 wt % of FR

including gas-phase effects, endothermic effects and slightly condensed-phase effects.

Mechanical properties

The loss factor (tan δ) curves of NC and FR/NCs are shown in Fig. 10a. It can be seen that only a glass transition temperature (T_g) is identified for DMMP/NC and (DMMP/CP = 8/2)/NC, which is attributed to the good compatibility between DMMP and NC. In addition, the T_g of (DMMP/CP = 8/2)/NC is significantly lower than that of NC. As reported, a decrease of T_g in principle increases the toughness of polymer [47]. This may be because of the increased free volume of the NC-rich phase, in which some DMMP molecules gain access to the void space of the NC structure [48]. Therefore, the above results indicate that the DMMP is a kind of organophosphorus flame retardant and also acts as a plasticizer, which can be used to improve the brittleness of NC.

Figure 10b presents the stress-strain curves of NC and FR/NCs, and the related data are shown in Table 4. As it can be seen, the tensile moduli, tensile strength and the elongation at break of (DMMP/CP = 8/2)/NC is higher than that of CP/NC and DMMP/NC, suggesting there may exist a synergistic effect between DMMP and CP. What is more, the elongation at break of (DMMP/CP = 8/2)/NC reaches the maximum value among all samples, showing the synergistic plasticization effect. As we know, the material brittleness is inversely proportional to the elongation at break [12]. Therefore, the co-plasticization of DMMP and CP can be a solution for the ductility improvement and the brittleness reduction of NC-based materials.

The SEM images of both NC and FR/NCs cross-sections are shown in Fig. 11. It is noteworthy that all FR/NCs present plastic flow property, which is very different from NC. This phenomenon can further confirm the plasticizing effects of the flame retardants.

CONCLUSIONS

Flame retardant low-nitrogen nitrocelluloses (FR/NCs) incorporating dimethyl methylphosphonate (DMMP) and long-chain chlorinated paraffin (CP) were prepared by blending method. This study successfully showed

that the combination of DMMP and CP could provide a self-extinguishing behavior, a phosphorus-chlorine synergistic effect and a great improvement of the flame retardancy of NC. Concretely, when the weight ratio of DMMP/CP was 8/2, the *LOI* value was increased from 17.6 % of NC to 28.4 %, and a HB rating was reached. Furthermore, the index of fire performance possessed the highest value (0.015 m^2s/kW) and the average effective heat of combustion got the lowest value (2.0 MJ/kg). All these values are superior to that of the samples obtained by adding DMMP or CP alone. DSC results presented the endothermic effect of DMMP/CP = 8/2, and TGA-FTIR results showed the gas-phase effect of flame retardancy due to the release of quenching free radicals. In addition, the formation of solid char layer, the retained char residues containing phosphorus and chlorine elements and the formation of char residues with higher graphitization degree all revealed the condensed-phase effect of flame retardancy for (DMMP/CP = 8/2)/NC sample. All the phenomena showed a comprehensive multi-flame retardancy mechanism including gas-phase effects, endothermic effects and slightly condensed-phase effects during the combustion. In addition, the obviously improved elongation at break of (DMMP/CP = 8/2)/NC was achieved through the synergistic plasticization effect between DMMP and CP.

This work was financially supported by National Key R&D Program of China (No. 2016YFB0302100) and National Natural Science Foundation of China (No. 21474008).

REFERENCES

[1] Wang Z., Zhang T., Zhao B., Luo Y.: *Polymer International* **2017**, *66*, 705. http://dx.doi.org/10.1002/pi.5312
[2] Shin K.Y., Tak Y.J., Kim W.G. *et al.*: *ACS Applied Materials and Interfaces* **2017**, *9*, 13 278. http://dx.doi.org/10.1021/acsami.7b00257
[3] Su X., Chen Z., Zhang Y.: *Chemical Papers* **2017**, *71*, 2145. http://dx.doi.org/10.1007%2Fs11696-017-0207-7
[4] Secor E.B., Gao T.Z., Islam A.E. *et al.*: *Chemistry of Materials* **2017**, *29*, 2332. http://dx.doi.org/10.1021/acs.chemmater.7b00029
[5] Santamaría B., Laguna M.F., López-Romero D. *et al.*: *Sensors* **2017**, *17*, 1158. http://dx.doi.org/10.3390/s17051158
[6] Zhang X., Weeks B.L.: *Journal of Hazardous Materials* **2014**, *268*, 224. http://dx.doi.org/10.1016/j.jhazmat.2014.01.019
[7] Yoon J., Lee J., Choi B. *et al.*: *Nano Research* **2017**, *10*, 87. http://dx.doi.org/10.1007/s12274-016-1268-6
[8] Rychlý J., Lattuati-Derieux A., Matisová-Rychlá L. *et al.*: *Journal of Thermal Analysis and Calorimetry* **2012**, *107*, 1267. http://dx.doi.org/10.1007/s10973-011-1746-8
[9] Wei R., He Y., Liu J. *et al.*: *Materials* **2017**, *10*, 316. http://dx.doi.org/10.3390/ma10030316
[10] Książczak A., Wolszakiewicz T.: *Journal of Thermal Analysis and Calorimetry* **2002**, *67*, 751. http://dx.doi.org/10.1023/A:1014333627793
[11] Yang X., Wang Y., Li Y. *et al.*: *Polimery* **2017**, *62*, 576. http://dx.doi.org/10.14314/polimery.2017.576
[12] Yang X., Li Y., Wang Y. *et al.*: *Journal of Polymer Research* **2017**, *24*, 50. http://dx.doi.org/10.1007/s10965-017-1203-x
[13] Shi X., Liao F., Ju Y. *et al.*: *Fire Materials* **2017**, *41*, 362. http://dx.doi.org/10.1002/fam.2389
[14] Ma T., Guo C.: *Journal of Analytical and Applied Pyrolysis* **2017**, *124*, 239. http://dx.doi.org/10.1016/j.jaap.2017.02.001
[15] Xiang H.F., Xu H.Y., Wang Z.Z., Chen C.H.: *Journal of Power Sources* **2007**, *173*, 562. http://dx.doi.org/10.1016/j.jpowsour.2007.05.001
[16] Feng F., Qian L.: *Polymer Composites* **2014**, *35*, 301. http://dx.doi.org/10.1002/pc.22662
[17] Wang C.Q., Lv H.N., Sun J., Cai Z.S.: *Polymer Engineering and Science* **2014**, *54*, 2497. http://dx.doi.org/10.1002/pen.23794
[18] Wang C.Q., Ge F.Y., Sun J., Cai Z.S.: *Journal of Applied Polymer Science* **2013**, *130*, 916. http://dx.doi.org/10.1002/app.39252
[19] Brandsma S.H., Van M.L., O'Brien J.W. *et al.*: *Environmental Science and Technology* **2017**, *51*, 3364. http://dx.doi.org/10.1021/acs.est.6b05318
[20] U. Laboratories. http://www.dxdlw.com/bbsupfile/2014/12/10/1501300105/UL94-2014.pdf (access date 11.07.2017)
[21] Zhao H.B., Liu B.W., Wang X.L. *et al.*: *Polymer* **2014**, *55*, 2394. http://dx.doi.org/10.1016/j.polymer.2014.03.044
[22] Yan H., Zhao Z., Ge W. *et al.*: *Industrial and Engineering Chemistry Research* **2017**, *56*, 8408. http://dx.doi.org/10.1021/acs.iecr.7b01896
[23] Feng J., Hao J., Du J., Yang R.: *Polymer Degradation and Stability* **2012**, *97*, 605. http://dx.doi.org/10.1016/j.polymdegradstab.2012.01.011
[24] Liu J., Yu Z., Chang H. *et al.*: *Polymer Degradation and Stability* **2014**, *103*, 83. http://dx.doi.org/10.1016/j.polymdegradstab.2014.03.014
[25] Laoutid F., Lorgouilloux M., Bonnaud L. *et al.*: *Polymer Degradation and Stability* **2017**, *136*, 89. http://dx.doi.org/10.1016/j.polymdegradstab.2016.12.013
[26] Lenża J., Merkel K., Rydarowski H.: *Polymer Degradation and Stability* **2012**, *97*, 2581. http://dx.doi.org/10.1016/j.polymdegradstab.2012.07.010
[27] Tang W., Zhang S., Sun J. *et al.*: *Thermochimica Acta* **2017**, *648*, 1.

http://dx.doi.org/10.1016/j.tca.2016.12.007
[28] Jiao Y., Wang X., Wang Y. *et al.*: *Journal of Macromolecular Science Part B* **2009**, *48*, 889. http://dx.doi.org/10.1080/00222340903028969
[29] Wang G., Nie Z.: *Polymer Degradation and Stability* **2016**, *130*, 143. http://dx.doi.org/10.1016/j.polymdegradstab.2016.06.002
[30] Ma Y., Wang J., Xu Y. *et al.*: *Journal of Applied Polymer Science* **2015**, *132*, 42 730. http://dx.doi.org/10.1002/app.42730
[31] Liu X., Zhou Y., Ha J., Du J.: *Journal of Applied Polymer Science* **2015**, *132*, 41 846. http://dx.doi.org/10.1002/app.41846
[32] Du J., Guan H., Song D.M., Liu H.: *Infrared Physics and Technology* **2017**, *80*, 21. http://dx.doi.org/10.1016/j.infrared.2016.10.001
[33] Zhao X., Guerrero F.R., Llorca J., Wang D.Y.: *ACS Sustainable Chemistry and Engineering* **2016**, *4*, 202. http://dx.doi.org/10.1021/acssuschemeng.5b00980
[34] Si M., Feng J., Hao J. *et al.*: *Polymer Degradation and Stability* **2014**, *100*, 70. http://dx.doi.org/10.1016/j.polymdegradstab.2013.12.023
[35] Jia P., Zhang M., Liu C. *et al.*: *RSC Advances* **2015**, *5*, 41 169. http://dx.doi.org/10.1039/c5ra05784a
[36] Panayotov D.A., Morris J.R.: *Journal of Physical Chemistry C* **2009**, *113*, 15 684. http://dx.doi.org/10.1021/jp9036233
[37] Kanan S.M., Waghe A., Jensen B.L., Tripp C.P.: *Talanta* **2007**, *72*, 401. http://dx.doi.org/10.1016/j.talanta.2006.10.046
[38] Park E.J., Han S.W., Jeong B. *et al.*: *Applied Surface Science* **2015**, *353*, 342. http://dx.doi.org/10.1016/j.apsusc.2015.06.122
[39] Zheng Y., Song J., Cheng B., Fang X.: *Fibers and Polymers* **2016**, *17*, 1. http://dx.doi.org/10.1007/s12221-016-5394-2
[40] Camino G., Costa L.: *Polymer Degradation and Stability* **1980**, *2*, 23. http://dx.doi.org/10.1016/0141-3910(80)90013-0
[41] Costa L., Camino G.: *Polymer Degradation and Stability* **1985**, *12*, 117. http://dx.doi.org/10.1016/0141-3910(85)90070-9
[42] Zhang Y., Ni Y.P., He M.X. *et al.*: *Polymer* **2015**, *60*, 50. http://dx.doi.org/10.1016/j.polymer.2015.01.030
[43] Jiao X., Zhang L., Qiu Y., Guan J.: *Colloids and Surfaces A* **2017**, *529*, 292. http://dx.doi.org/10.1016/j.colsurfa.2017.05.094
[44] Yuan B., Wang B., Hu Y. *et al.*: *Composites Part A: Applied Science and Manufacturing* **2016**, *84*, 76. http://dx.doi.org/10.1016/j.compositesa.2016.01.003
[45] Bohn M.A.: *Journal of Thermal Analysis and Calorimetry* **2001**, *65*, 103. http://dx.doi.org/10.1023/A:1011524517975
[46] WO 2015/049286 A2 (2015).
[47] Zheng T., Ni X.: *RSC Advances* **2016**, *6*, 57 122. http://dx.doi.org/10.1039/C6RA08178A
[48] Zhang W., Li X., Guo X., Yang R.: *Polymer Degradation and Stability* **2010**, *95*, 2541. http://dx.doi.org/10.1016/j.polymdegradstab.2010.07.036

Received 12 XII 2017.